NREL/TP-411-5760 • UC Category: 271 • DE93018220

Research on Stable, High-Efficiency Amorphous Silicon Multijunction Modules

Annual Subcontract Report 1 November 1992 – 31 May 1993

M. Ghosh, F. Kampas, J. Xi
Advanced Photovoltaic Systems
Princeton, New Jersey

NREL technical monitor: W. Luft

National Renewable Energy Laboratory
1617 Cole Boulevard
Golden, Colorado 80401-3393
Operated by Midwest Research Institute
for the U.S. Department of Energy
under Contract No. DE-AC02-83CH10093

Prepared under Subcontract No. ZM-2-11091-1

September 1993

NOTICE

Printed in the United States of America
Available from:
National Technical Information Service
U.S. Department of Commerce
5285 Port Royal Road
Springfield, VA 22161

Price: Microfiche A01
Printed Copy A03

Codes are used for pricing all publications. The code is determined by the number of pages in the publication. Information pertaining to the pricing codes can be found in the current issue of the following publications which are generally available in most libraries: *Energy Research Abstracts (ERA)*; *Government Reports Announcements and Index (GRA and I)*; *Scientific and Technical Abstract Reports (STAR)*; and publication NTIS-PR-360 available from NTIS at the above address.

Printed on recycled paper

Preface

This report describes work done at Advanced Photovoltaic Systems during the first half of Phase II of the NREL contract "Research on Stable, High-Efficiency Modules." The goal of the contract is the development of same bandgap, amorphous silicon, tandem-junction modules. The research involved a coordinated effort among two groups in the Research Department of Advanced Photovoltaic Systems: the Device Group and the Module Group. The approach taken was to develop improved semiconductor device structures in the Device Group. The results of their efforts were then transferred to the Module Group. The Module Group is responsible for scale up of the small-area device results and for optimization of module processing techniques. In addition to the two groups in the Research Department, there was also a contribution from APS' Manufacturing Department, which allowed the use of some of their facilities.

Executive Summary

OBJECTIVES

The principal objective of the research described in this report is the development of stable, high-efficiency two-terminal, similar-bandgap, amorphous silicon multijunction photovoltaic modules. Related objectives involve developing cost-effective fabrication processes for these modules and obtaining data on the reliability of the modules. The major goal of the three-phase research program is the demonstration of a stable, aperture-area efficiency of at least 10% for two-terminal, similar-bandgap, amorphous silicon multijunction modules having an aperture area greater than 900 cm^2. The major goal of the second phase of the contract is demonstration of stable aperture-area efficiency of 8% for such modules. This report covers the first half of that phase.

APPROACH

The approach taken involved deposition and characterization of individual semiconductor and non-semiconductor films, tandem-junction devices, and tandem-junction modules. Deposition techniques used were Plasma Enhanced Chemical Vapor Deposition for the various silicon films and layers and magnetron sputtering for the non-semiconductor films and layers. Individual layers were characterized by dark and photoconductivity (where appropriate), by thickness uniformity measurements, and by optical characterization (where appropriate). Devices were characterized for initial and light-soaked characteristics using I-V and quantum efficiency measurements. Modules were characterized by I-V measurements.

SUMMARY OF RESULTS

Considerable effort was devoted to reconciling the contradictory requirements on the p2 layer, the p layer of the second stack of the tandem junction structure. The best "tunnel junction" (the contact between the two stacks) was obtained when the p2 layer had a relatively low band gap. However, that resulted in reduced voltage and current from the second stack. The use of a very thin (< 1 nm thick) p^+ (no carbon) layer between the n1 layer and a high band gap p2 layer results in a good tunnel junction and results in normal current and voltage from the second stack.

Table of Contents

List of Figures

List of Tables

Semiconductor Materials Research

Introduction

Semiconductor layers for individual film studies and for device and module studies were deposited in three different deposition systems. The first of these, the "B" system, is a single-chamber, small-area deposition system which uses a 5.1 cm x 5.1 cm (2" x 2") substrate. Typically, a number of 1 cm^2 devices would be prepared from each run. The second system, the "A" system, has two deposition chambers and a load-lock. Like the "B" system, it uses a 5.1 cm x 5.1 cm substrate. The "A" and "B" systems were used for depositions of semiconductor layers and single-junction and tandem-junction devices.The third system, the "D2" system, can hold four substrates up to 33 cm x 33 cm (13" x 13") in size. Separate layer and tandem-junction module depositions were performed in this system. Typically, two substrates are processed into modules and two are processed into diagnostic 1 cm^2 devices in a module deposition run.

I Layers

A number of I-layer depositions were performed in the D2 system. This phase of the contract sets a goal of a thickness uniformity of ± 7% over 900 cm^2 for an approximately 400 nm thick i-layer with 1.7-1.8 eV optical band gap with the same quality as required for Phase I, a value for the photosensitivity (photoconductivity at 1000 W/m^2 divided by dark conductivity) > 10^5. The allowed deviation in each direction is defined as twice the coefficient of variation. (The coefficient of variation is the standard deviation divided by the average.)

Results of thickness measurements are shown in Figure 1 for run D2-218, which had an average thickness of 246.8 nm and a standard deviation in thickness of 12.9 nm. Therefore, two times the coefficient of variation is 10.5%, somewhat higher than the goal for the end of the phase. The value of the photosensitivity is 3.3 x 10^5. The top of the electrode is shown in the lower left of the figure. The increase in film thickness going from the top to the bottom is presumably due to gas phase polymerization, resulting in the production of higher silanes, which causes a higher deposition rate.

N Layers

This phase of the contract requires a ±10% uniformity over an area of 900 cm^2 for an n^+ layer of 100 nm thickness. Results are shown in Figure 2 for a microcrystalline n-layer deposited in the D2 system. The average thickness of the film is 108 nm and the standard deviation in the film thickness is 7.2 nm. This gives a value for twice the coefficient of deviation of 13.3%. The orientation of the figure is the same as in the previous figure: the top of electrode is shown at the lower left. The thicker region near the top of the electrode is believed to be due to a discharge to the metallic gas inlet of the box carrier. A modified design which eliminates that problem has been developed and was used for the i-layer deposition described earlier.

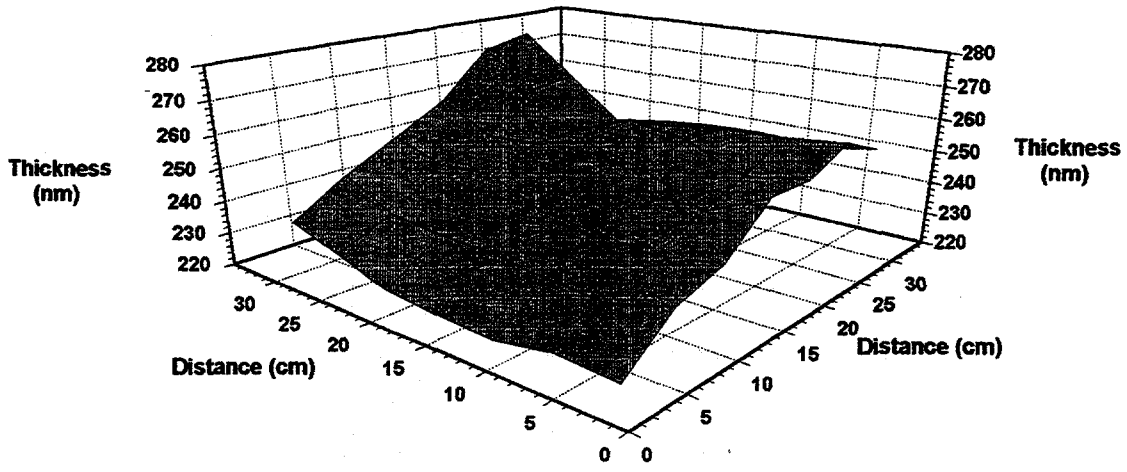

Figure 1. Thickness distribution of an i layer deposited in the D2 system.

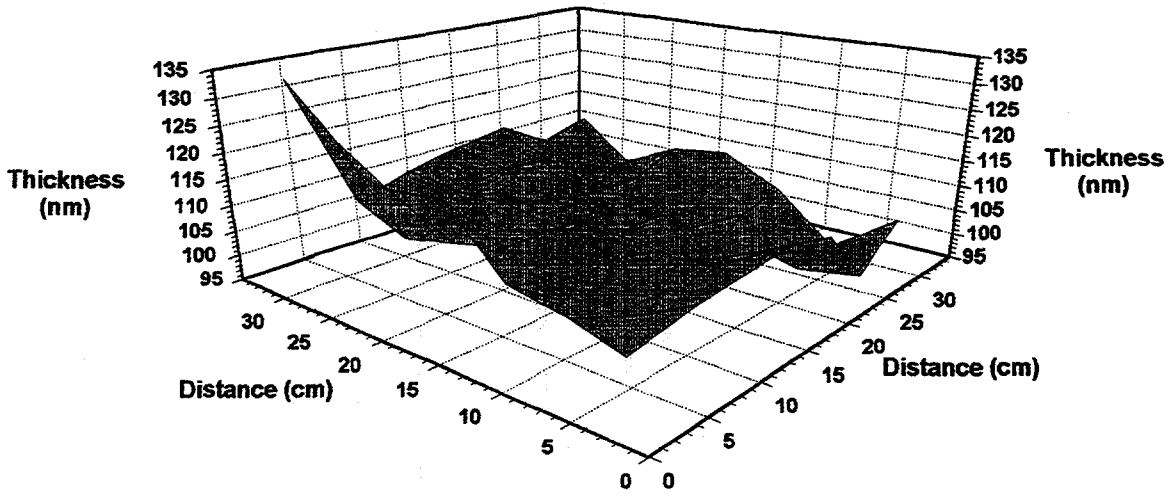

Figure 2. Thickness distribution of an n layer deposited in the D2 system.

Non-Semiconductor Materials Research

Tin Oxide

High-haze, high-transmission, low sheet-resistivity transparent-conducting-oxide-coated glass is essential for achieving high efficiency amorphous silicon devices and modules. One goal of this phase of the contract is the achievement of $\geq$ 82% integrated transmittance and $\leq$ 5 ohms/square sheet resistance for SiO_2 / SnO_2-coated glass with a resistance non-uniformity $\leq$ 10% over 900 cm^2 and optimized diffuse transmission. APS' tin oxide research program was placed "on hold" part way through the first half of this phase of the contract, due to limited resources. Consequently, no improvement was obtained over the best result from Phase I of the contract. This was 7.5 ohms/square sheet resistance (with 5% non-uniformity) and 81.4% transmittance, over 900 cm^2.

Zinc Oxide Back Reflector

Sputtered zinc oxide was used as a back reflector to increase the red response and short-circuit current density of tandem-junction devices. The goal in this phase of the contract for this activity was the demonstration of a 17% increase in short-circuit current density compared to that obtained with Al back metallization for a 1 cm^2 tandem-junction cell through use of an enhanced back reflector. This goal was achieved early in Phase II, on run B-609. The results (before light soaking) are shown in Table 1. The device with the ZnO/Ag/Al back reflector had a 20.8% higher short-circuit current density than the device with the Ag/Al back reflector. (Ag/Al back reflectors typically give 3% higher short-circuit current density values than do Al back reflectors.) It should be noted that the use of a ZnO back reflector typically gives a short-current density increase of around 1 mA/cm^2.

Table 1. ZnO Back Reflector on a 1 cm^2 Tandem-junction Device.

Back Reflector	V_{oc} (Volts)	J_{sc} (mA/cm^2)	Fill Factor	Efficiency (%)
ZnO/Ag/Al	1.570	7.90	.686	8.50
Ag/Al	1.563	6.54	.696	7.12

Device Research

One of the two major milestones of the second phase of the contract is a 1-cm^2 tandem-junction device with a stabilized efficiency of 9.0% or more. The stabilized efficiency is defined as the efficiency after 600 hours of exposure to 1000 W/m^2 of light with an AM1.5 spectrum, with the device being held at a temperature of 50 ^{o}C. The best result to date was obtained for run B-685. Its parameters as a function of light-soaking time are shown in Table 2. The j-v curves of the device from run B-685 at the various light-soaking times are shown in the Figure 3. The initial j-v curve shows a small kink near V_{oc}, indicating some series resistance due to the tunnel junction. This kink became larger on light soaking.

Table 2. Parameters of the best 1 cm^2 device.

hours light soaking	V_{oc} (Volts)	J_{sc} (mA/cm^2)	Fill Factor	Efficiency (%)	Series Resistance ($ohm\text{-}cm^2$)
0	1.661	7.96	.699	9.25	36.08
161	1.610	7.63	.608	7.47	53.29
254	1.605	7.65	.606	7.44	54.18
587	1.597	7.60	.602	7.31	57.85
708	1.567	7.61	.603	7.18	52.86

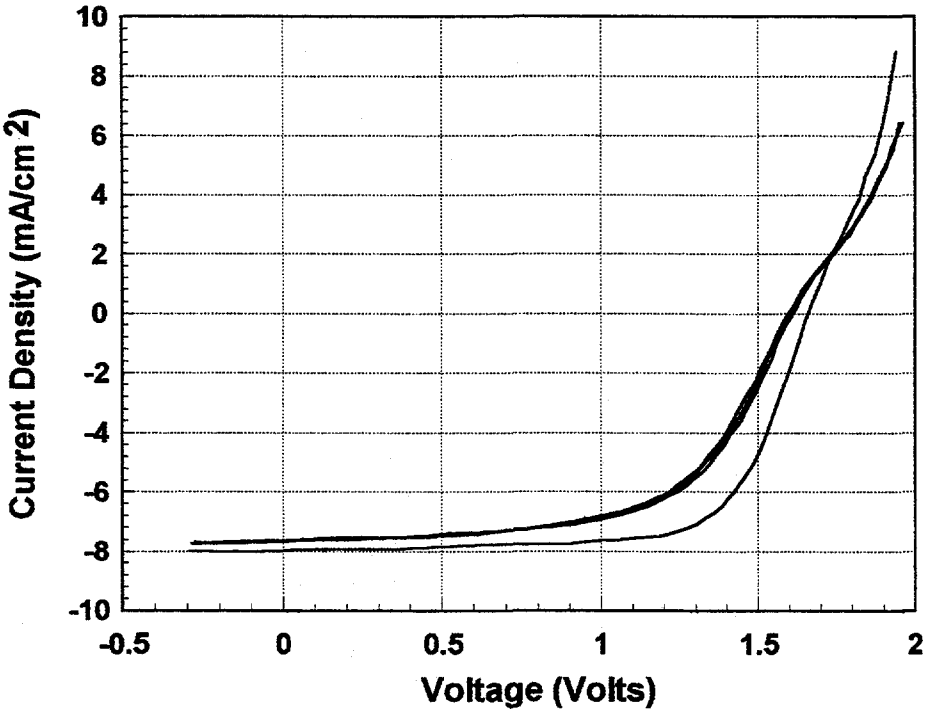

Figure 3. Effect of light soaking on the J-V Curve of run B-685.

The increase in series resistance and the related decrease in fill factor on light soaking occurred for all of the tandem devices which were light soaked. The extent of the increase varied for different devices. This is shown in Figure 4. The figure shows both the initial and stabilized fill factor and series resistance. The arrow indicates the change on light soaking.

Larger increases in series resistance and larger decreases in fill factor were observed for higher initial values of series resistance, even though there was no correlation between initial fill factor and initial series resistance. The correlation between initial series resistance and stabilized fill factor allows a crude estimate of the stabilized result from the initial values.

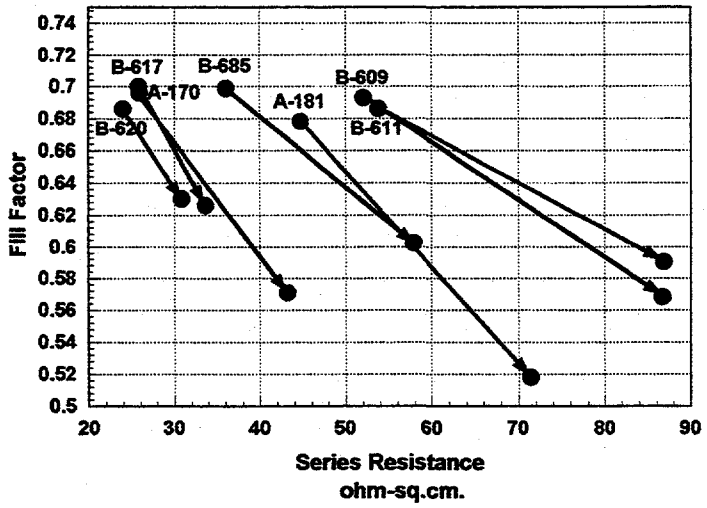

Figure 4. Effect of light soaking on fill factor and series resistance.

Run B-685, the device with the higher stabilized efficiency, did not have the highest stabilized fill factor. This is because there was an inverse correlation between stabilized fill factor and the values for stabilized open-circuit voltage and short-circuit current density. This is shown in Figure 5. The figure shows three separate plots, combined into three faces of a rectangular solid. The three plots are fill factor vs J_{sc}; fill factor vs V_{oc}; and J_{sc} vs V_{oc}. The arrows connect the initial values of the parameters to the stabilized values in the three plots.

The data in the figure show a positive correlation between both initial and stabilized values of V_{oc} and J_{sc}. The data also show a negative correlation between stabilized fill factor and both stabilized V_{oc} and J_{sc}. These negative correlations result in a fairly low value for the stabilized efficiency because the devices with high stabilized V_{oc} and J_{sc} have low values of stabilized fill factor and vice versa.

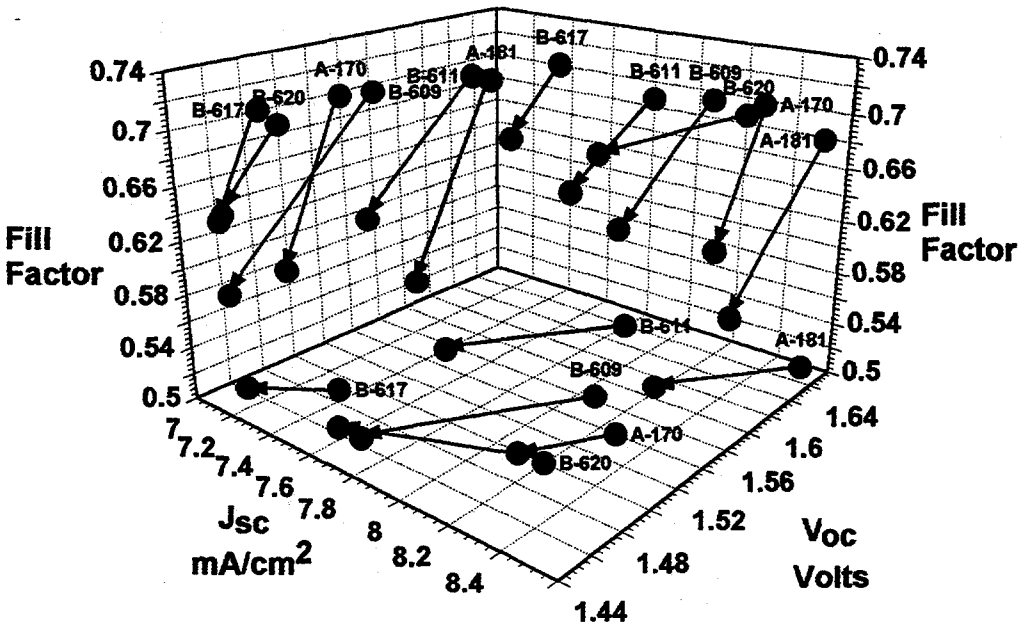

Figure 5. Effect of light soaking on V_{oc}, J_{sc}, and fill factor.

The positive correlation between V_{oc} and J_{sc} results from a variation in the band gap of the p2 layer, caused by different methane to silane ratios used in the deposition. Increased band gap of the p2 layer increases the amount of light entering the i2 layer, as well as increasing the built-in potential for the second stack. This is shown in Figure 6.

The decrease of stabilized fill factor with increasing carbon content of the p2 layer is more difficult to understand. One possible explanation is that increased band gap of the p2 layer increases the built in potential in the tunnel junction, resulting in higher resistivity. However, it is not clear why that effect should only lower the stabilized fill factor and not the initial fill factor. Another possibility is that a poor tunnel junction causes higher carrier densities in the i layers, resulting in more Staebler-Wronski degradation.

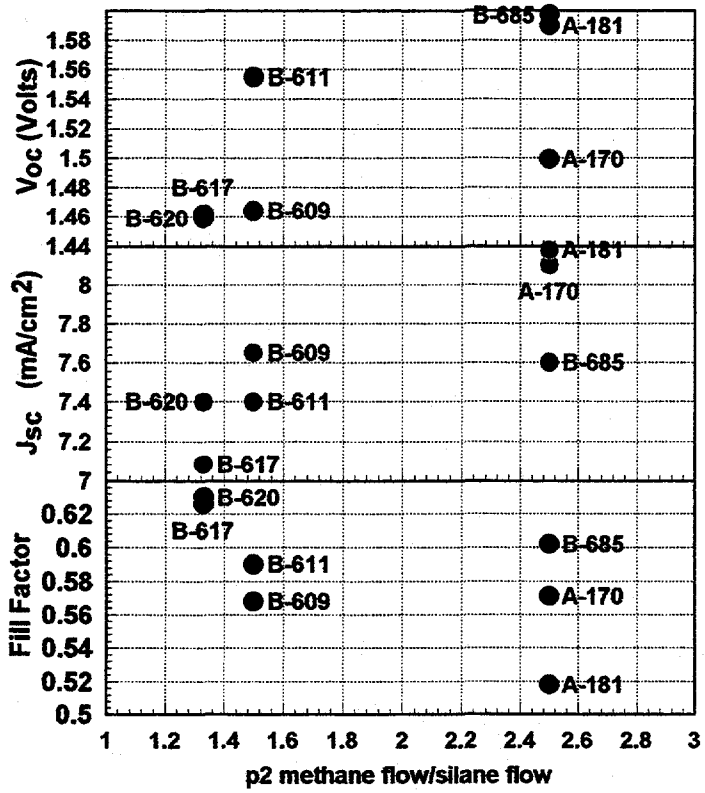

Figure 6. Effect of p2 composition of device parameters.

The data in the figures show that device B-685 had a relatively high stabilized fill factor as well as a relatively high V_{oc}. The reason for this can be understood by looking at the detailed structure of the device. Figure 7 shows the effect of changing tunnel junction structure on the stabilized V_{oc} and fill factor of a number of devices made in the B system. The code next to each point describes the components of the tunnel junction. The n1 layer is either amorphous (a) or microcrystalline (uc). The p2 layer can be low carbon (-c) or high carbon (+c). It can also be either thin (-d) or thick (+d). Furthermore, one sample (run B-685) had a p^+ layer (a boron doped p layer with no carbon) between n1 and p2. The italicized words next to the arrows show the effect of changing various components of the tunnel junction structure. For example, increasing the thickness of the p2 layer (increase d) lowers stabilized fill factor with either no or a small increase in stabilized V_{oc}. Replacing the amorphous n1 layer by a microcrystalline n layer has almost no effect for a thin, low carbon p2 layer, but results in a decrease in stabilized fill factor and V_{oc} for a thick, low carbon p2 layer. This effect may indicate that the quality of the microcrystalline n1 layer is not adequate. Films on glass using the microcrystalline n1 layer conditions have high lateral conductivities. However, films deposited on amorphous i layers using those conditions do not.

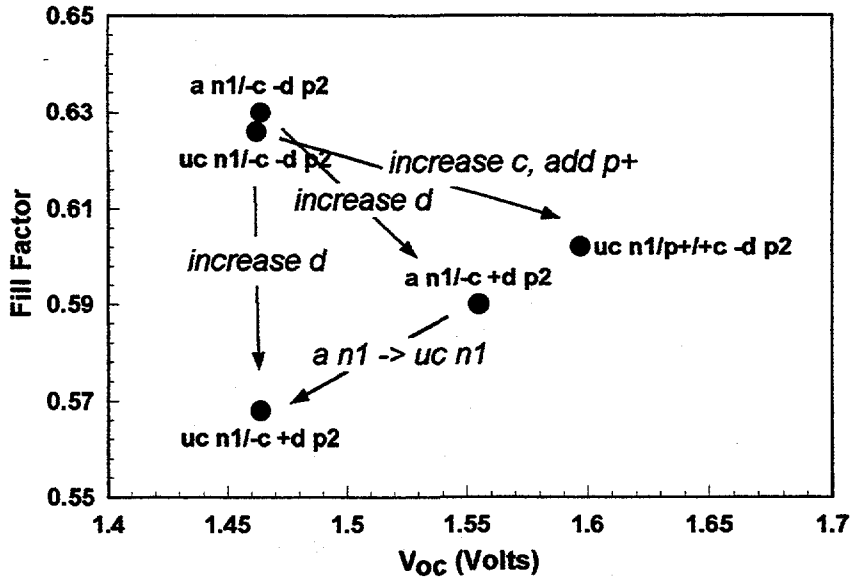

"a" refers to an amorphous n1 layer
"uc" refers to a microcrystalline n1 layer
"+c" refers to a high carbon p2 layer
"-c" refers to a low carbon p2 layer
"+d" refers to a 60 Angstrom p2 layer
"-d" refers to a 40 Angstrom p2 layer
"p+" refers to a 5 Angstrom no carbon p layer

Figure 7. Effect of tunnel junction structure on device fill factor and V_{oc}.

Module Research

The second major milestone of the second phase of the contract is the demonstration of a tandem module with an aperture-area efficiency ≥ 8.0% after 600 hours of light soaking. The aperture area of the module is required to be greater than 900 cm^2, and the active-area loss due to laser scribing is required to be less than 4%. The best result obtained was for run D2-185. The effect of light soaking on the module parameters is shown in Table 3. Short-circuit current density and efficiency are given on an aperture area basis.

Table 3. Parameters of the Best Module.

hours of light soaking	V_{oc} /cell Volts	J_{sc} mA/cm^2	Fill Factor	Efficiency %	Series Res. ohm-cm^2
0	1.486	6.56	.67	6.49	21
24	1.537	6.34	.64	6.21	24
289	1.551	6.39	.61	6.39	29
793	1.542	6.36	.59	5.79	31

The increase in V_{oc} on light soaking indicates that the doped layers are below optimum thickness for development of the built-in potential of the two stacks. However, modules with thicker doped layers did not have as high a value for stabilized efficiency. This is shown in the Table 4, which gives results for diagnostic 1 cm^2 devices made in a number of tandem junction depositions. The n1 layers of the devices were microcrystalline. Both amorphous and microcrystalline n2 layers were used. The type used is given in the table.

Table 4. Parameters of Diagnostic Devices.

Run	p1 dep. time sec.	n1 dep. time min.	type of n2 layer	light soak time hour	V_{oc} / cell Volt	J_{sc} mA/ cm^2	FF	Eff. %	Ser. Res. ohm - cm^2
179	80	20	μxtal	0	1.62	6.20	.64	6.48	25
179	80	20	μxtal	610	1.57	6.16	.63	6.08	31
180	80	15	μxtal	0	1.54	6.43	.68	6.71	37
180	80	15	μxtal	610	1.54	6.18	.63	6.01	28
185	50	12	amo	0	1.46	7.11	.69	7.14	23
185	50	12	amo	800	1.52	6.83	.59	6.1	34
187	60	12	amo	0	1.44	6.82	.68	6.71	25
187	60	12	amo	590	1.48	6.54	.60	5.82	37

The results in Table 4 do not give a clear indication of the effect of the changes in the p1,n1, and n2 layers, as the changes were not done in a systematic fashion. Therefore, the "design of experiments"

technique was used to set up a systematic set of experiments to optimize the layers, starting with the p1 layer. Eight experiments were performed in which two different values of four parameters of the p1 layer were tested. These four parameters were pressure, power, deposition time, and methane-to-silane ratio. A twelve minute microcrystalline n1 layer and an amorphous n2 layer were used. Some initial results and 300 hour light soaked results have been obtained and are presented in Table 5, for 1 cm^2 diagnostic cells, with ZnO/Al back reflectors.

Table 5. Efficiencies for Various p1 Deposition Conditions.

Efficiency (%): initial 300 hour		pressure = 350 mTorr		pressure = 500 mTorr	
		power = 20 Watts	power = 30 Watts	power = 20 Watts	power = 30 Watts
time = 50 seconds	$[CH_4]/[SiH_4]$ = 1.0	7.48			7.35 6.55
	$[CH_4]/[SiH_4]$ = 1.5		7.2	7.07	
time = 70 seconds	$[CH_4]/[SiH_4]$ = 1.0		7.07	7.45 6.35	
	$[CH_4]/[SiH_4]$ = 1.5	7.56 6.42			6.68

A module made in the same run as the 1 cm^2 devices with the highest efficiency at 300 hours (upper right hand corner of the table) had an initial aperture area efficiency of 7.03% and an efficiency of 6.14% after 300 hours of light soaking. When the cells from the set of experiments have completed 600 hours of light soaking, a new set of experiments for p1 layer optimization will be performed. In the mean time, similar optimization experiments will be done on other parts of the tandem cell structure.

Document Control Page	1. NREL Report No. NREL/TP-411-5760	2. NTIS Accession No. DE93018220	3. Recipient's Accession No.

4. Title and Subtitle
Research on Stable, High-Efficiency Amorphous Silicon Multijunction Modules

5. Publication Date
September 1993

6.

7. Author(s)
M. Ghosh, F. Kampas, J. Xi

8. Performing Organization Rept. No.

9. Performing Organization Name and Address
Advanced Photovoltaic Systems
Princeton, New Jersey 08543

10. Project/Task/Work Unit No.
PV341101

11. Contract (C) or Grant (G) No.
(C) ZM-2-11091-1
(G)

12. Sponsoring Organization Name and Address
National Renewable Energy Laboratory
1617 Cole Blvd.
Golden, CO 80401-3393

13. Type of Report & Period Covered
Technical Report
1 November 1992 - 31 May 1993

14.

15. Supplementary Notes
NREL technical monitor: W. Luft

16. Abstract (Limit: 200 words)

This report describes progress made in the first half of Phase II of a three-phase program to develop high-efficiency, same-band-gap, amorphous-silicon, tandem-junction modules. Results for both 1-cm^2 devices and 0.3-m (0.09-m^2) modules are given. Considerable effort was devoted to finding a device structure and layer conditions that reconcile the conflicting requirements of a good "tunnel junction" contact between the two stacks and a high-efficiency device. High-band-gap p_2 layers, which enable good voltage and current from the second stack, were found to result in poor tunnel junctions. The best results were obtained by using a thin (< 1-nm-thick) p^+ layer (no carbon) between the n_1 and p_2 layers of the device.

17. Document Analysis
a. Descriptors
high efficiency ; amorphous silicon ; modules ; photovoltaics ; solar cells

b. Identifiers/Open-Ended Terms

c. UC Categories
271

18. Availability Statement
National Technical Information Service
U.S. Department of Commerce
5285 Port Royal Road
Springfield, VA 22161

19. No. of Pages
19

20. Price
A03